

Research Article

Design and Implementation of Plastic Deformation Behavior by Cartesian Impedance Control Based on Maxwell Model

Le Fu  and Jie Zhao 

State Key Laboratory of Robotics and System, School of Mechanical Engineering, Harbin Institute of Technology, Harbin 150080, China

Correspondence should be addressed to Le Fu; 14b308007@hit.edu.cn

Received 14 August 2018; Accepted 7 November 2018; Published 2 December 2018

Guest Editor: Junpei Zhong

Copyright © 2018 Le Fu and Jie Zhao. This is an open access article distributed under the Creative Commons Attribution License, which permits unrestricted use, distribution, and reproduction in any medium, provided the original work is properly cited.

Compliance has become one prerequisite of robots designed to work in complex operation environment where dynamic and uncertain physical contact or impact takes place frequently and even intentionally. Impedance control is a typical compliant control methodology. Standard impedance control is based on dynamics described by a spring and damper model connected in parallel way, which endues the robot an elastic behavior. In contrast, plastic deformation can be realized by Maxwell model in which spring and damper connect in series. In this study, a novel Cartesian impedance controller is constructed based on the Maxwell model. Implementation in a robot manipulator is executed to validate and analyze the proposed control law. A plastic deformation behavior of the robot manipulator is produced and certain extent compliance is achieved under the unpredictable impact or contact force exerted by human or other environment objects.

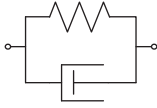
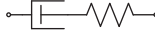
1. Introduction

A rapid increase in the opportunity of robots' physical interaction with complex environment, including humans, other robots, and operational objects has occurred because of the tendency that robots break through the confined spaces and structured environments. One major challenge is the provision of innovative solutions to deal with the situations in which robots run in complex operation environments. Therefore, compliance has become one of a few prerequisites of robots since it can deal with a certain extent uncertainty and complexity, especially the prevention of damage to robot itself and environment. In general, there are two categories of compliance. One is mechanical or passive compliance, including remote center compliance, which is also called RCC device [1]. Other mechanisms have been developed to implement a sense of mechanical softness, such as variable stiffness joint, also called VS-joint [2, 3], pneumatic artificial muscle actuators [4]. In some literatures, these mechanisms are also referred as compliant design for intrinsic safety [5].

The other way of compliance is software servo control or active compliance. Impedance control is a typical compliant control methodology, which adjust the inertia, viscosity, and elasticity to achieve a dynamic relationship

between displacement and external force. This original idea of a impedance model used for controlling the interaction between manipulator and environment dates back to the works [6, 7]. Several different approaches to implement this control method have been proposed from a variety of perspectives: feedback from positions and velocities without the need for force sensors [8] and the adjustment of joint-independent compliance to set the compliance of an end-effector [9]. For redundant manipulators, the use of null-space motion is the key to meet additional requirements with respect to the desired behavior [10]. The design of null-space stiffness and damping has been well researched in the task space and joint space [11]. Impedance controller for flexible joint robots is proposed in [12, 13]. In their appealing works, both methods have a cascaded structure with an inner torque feedback loop and an outer impedance controller. In [14], learning impedance control is proposed for physical robot-environment interaction. The dynamics of the robot arm is governed to follow a target impedance model and the interaction control objective is achieved. A novel interface for human impedance adaptive skill transfer in a natural and intuitive manner is proposed by [15]. Besides, a DMP-based framework for robot learning and generalization of humanlike variable impedance skills is formulated in [16].

TABLE I: Two viscoelastic models.

Two models	Voigt model	Maxwell model
Illustration		
Motion equations (1-DOF case)	$m\ddot{x} + c\dot{x} + kx = f$	$m\ddot{x} + \frac{mk}{c}\dot{x} + kx = f + \frac{k}{c} \int f dt$
Overdamped condition	$c^2 > 4mk$	$c^2 < \frac{1}{4}mk$
Connection	Parallel	Series
Deformation	Elastic	Plastic

These impedance control methods mentioned above are based on a kind of viscoelastic model [17] which is called Voigt model that connects a spring and damper in parallel way. Therefore, a repulsive force is always generated because of the superior effect of spring. In other words, the spring is dominant in Voigt model. By contrast, there is another parallel-type viscoelastic model called Maxwell model. In [18], a visual absorber based on Maxwell model to realize a natural impact absorption is proposed. In their work, a shock absorber is constructed by a spring-based passive elastic body and a damping controlled joint connected in series. This 2-DOF robot receives the impact of a rolling down object without repelling it, which is called plastic behavior. A Maxwell model based impedance control law is proposed for smoothly receiving the impact of an incoming object in [19]. Simulations of the impact absorption with a robotic arm are executed using an open dynamics engine to validate and analyze the proposed control laws. However, to our knowledge, no practical robot platform implementation has been reported in literature works. Differences between simulation and practical implementation always exist, since simulation is a kind of simplification and approximation in most cases. Therefore, we propose a Cartesian impedance control scheme based on Maxwell model and implement it in a scenario where unknown contact between robot and other objects exists. Different from previous works, the design and implementation of our method remain in Cartesian space which is more closely related to the physical interaction between robot and environment than in joint space. The experiment results show that a plastic deformation behavior is realized when unknown contacts and impacts happen. Certain extent compliance is achieved under the unpredictable impact or contact force exerted by human or other environment objects. Our work shows a promising usage in some impact energy absorption tasks such as robot catching flying ball without repelling. And this kind of compliance may open a gate in human robot collaboration tasks to ensure the robot a more soft and passive contact with humans.

In this paper, we design a Cartesian impedance controller based on Maxwell model to realize a kind of plastic deformation behavior in a robot manipulator. First, the motion equations are given and dynamic properties of both models are described. After that, the existence of an equivalent transformation of the Maxwell model between the series

and parallel representations is emphasized. Next, a Cartesian impedance control law based on Maxwell model for multiple links robotic arms is proposed to achieve a plastic deformation behavior. Finally, the proposed methods are validated by experiments and discussions are given with an emphasis on differences between our method and standard impedance control. Attached video (available here) is given as a demonstration of our work.

2. Comparison of Two Models

The concept of viscoelastic models [17] dates back to early works in material and other scientific disciplines. There are two basic linear viscoelastic models: the Voigt model and the Maxwell model, as shown in Table 1. Motion equations and over-damped conditions of both models in one-dimensional case are also given. It is assumed that a mass of m , spring constant k , and damping or viscosity coefficient c are all lumped elements. The Voigt model, which connects a spring and damper in parallel, is suitable for representing elastic deformation, in which the displacement returns to zero when an external force is removed. In contrast, the Maxwell model, which connects a spring and a damper in series, is suitable for representing plastic deformation, in which the displacement does not return to zero, even when the external force is removed. That is why we call it plastic deformation.

The time-domain transient and steady state response of both viscoelastic models in different damping conditions, namely, under damping, critical damping, and over damping, are demonstrated in Figure 1. In one-dimensional case, the difference of dynamic properties of two viscoelastic models is shown in Figure 1. As can be seen from Figure 1(a), the deviation displacements converge to zero under different coefficients, namely, critical damping, over damping, and under damping, which means the system always returns to the original point. By contrast, the Maxwell model based system never returns to its original position. This phenomenon is called plastic deformation. In Figure 1(b), it is indicated that the rest or steady position can be changed from 0.5m to 2 m with different coefficients. Besides, the transient response is also determined by these system coefficients and is similar to the Voigt model case. Since most robot applications including our work have multiple joints, the motion equations and dynamic properties of multidimensional case are thoroughly studied as follows.

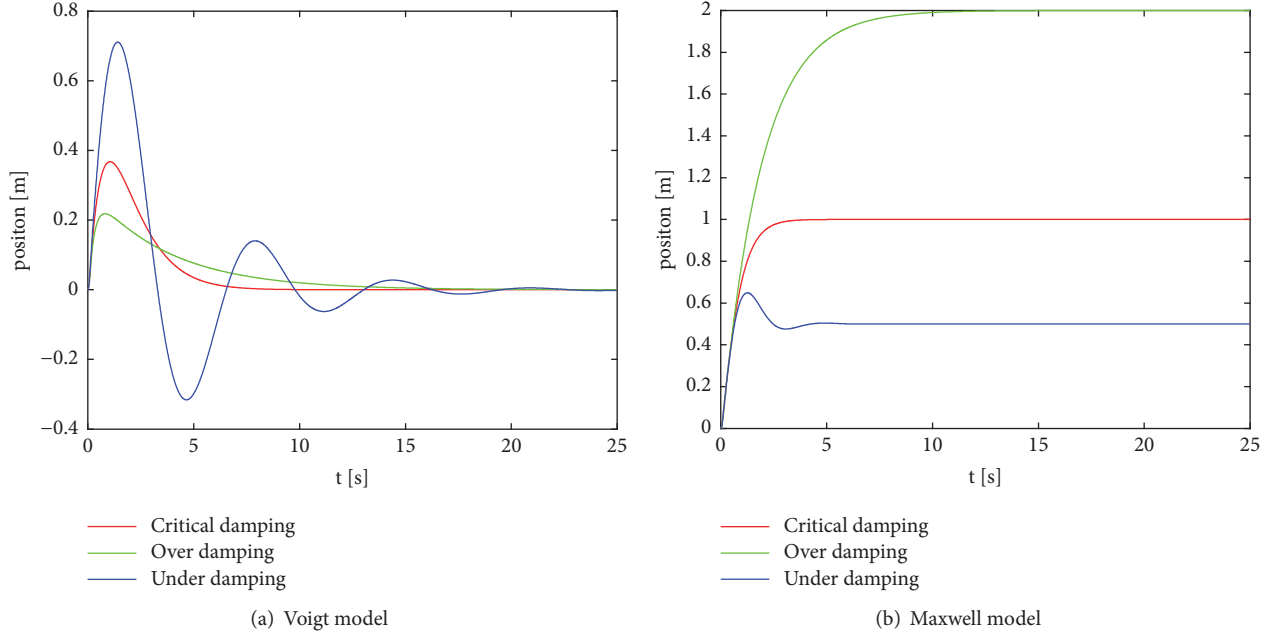


FIGURE 1: Dynamic properties depending on different coefficients of two viscoelastic models in one-dimensional case.

3. Modeling

3.1. Motion Equations. It is assumed that a mass of M , spring constant K , and viscosity coefficient C are lumped parameters, so the mass M is concentrated at the end-effector of robots. The displacement of the end-effector $x_e = x - x_0$ is varied with an external force F , where x and x_0 are current and neutral positions of the end-effector, respectively. Note that x_0 is a constant in set-point control of end-effector, also x_0 corresponds to the reference trajectory in common impedance control. For example, the titles for this document begin as follows:

- (i) Voigt Model: the well-known motion equation of standard impedance control can be expressed as follows:

$$M\ddot{x}_e + C\dot{x}_e + Kx_e = F \quad (1)$$

This typical second order differential equation describes the evolution of the end-effector when external force applied. And the displacement x_e converges to 0 if the external force $F \rightarrow 0$. Similar to one-dimensional case, the motion becomes over-damped under the condition of $c^2 > 4mk$.

- (ii) Maxwell Model: in the Maxwell model, the displacement of end-effector x_e is the sum of the displacements of spring and damper. The motion equation in this case can be represented as follows:

$$M\ddot{x}_e = F - K(x_e - p_e) \quad (2)$$

$$K(x_e - p_e) - C\dot{p}_e = 0 \quad (3)$$

where $p_e = p - p_0$ is the displacement of the damper and p and p_0 are current and neutral position of the

damper, respectively. Combining the two equations to eliminate p_e , the motion equation of the end-effector can be expressed by

$$M\ddot{x}_e + KC^{-1}M\dot{x}_e + Kx_e = F + KC^{-1} \int Fdt \quad (4)$$

Here, displacement of the end-effector x_e does not converge to 0 but to a position where the force balance of driven torque and the external force are exerted. This means the deformation caused by external forces is not elastic, but plastic. Intuitively, the damper does not necessary return to the original position, whereas the spring needs to return the neutral position. In the sense of conservation of energy, spring is a kind of elements which can store energy, but damper is a dissipation element. In our model, assume the friction is ignored, and when external force disappears, the spring releases the energy it stored and recovers to the original point, but the damper converts most energy into thermal energy. Moreover, this process is invertible, so the damper never comes back to original point like the spring. That is why plastic deformation happens.

3.2. Equivalent Transformation. According to the above second order differential equations, there is an equivalent transformation between these two model dynamics, through eliminating the intermediate variable p . The fact means that if the coefficients are appropriately adjusted, the Maxwell model can be transformed to the parallel expression, as shown in Figure 2, in which the damping term C is transformed to $KC^{-1}M$ and the integral term of external force $KC^{-1} \int Fdt$ is added. Moreover, when putting these models into controller

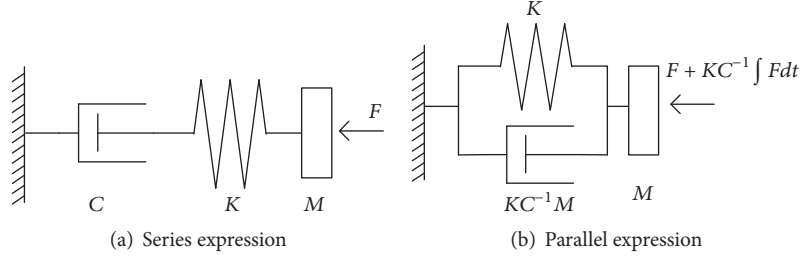


FIGURE 2: Equivalent transformation of the Maxwell model.

design, impedance control may realize the Maxwell model dynamic response if the parameters are properly adjusted like discussed above. In other words, a kind of equivalent transformation exists and the total behavior of each component does not depend on the order of the components. It should be noted that the torque input to the robot is required to compensate for the integral term of the external force when doing this equivalent transformation.

4. Controller Design

4.1. Contact Dynamics. The dynamics equation of a manipulator in joint space is as follows:

$$M(q)\ddot{q} + C(q, \dot{q})\dot{q} + g(q) = \tau + J^T F \quad (5)$$

where $M(q)$ is the inertia matrix in joint space and $C(q, \dot{q})$ and $g(q)$ are the Coriolis and Centrifugal forces and gravity, respectively. J is the Jacobian matrix, which represents the differential kinematics. τ is the driving forces or torques, and F is the external force exerted on the robot end-effector. Note that the friction is ignored or assume this term can be properly treated such as nonlinear compensation.

The Lagrange dynamics in joint space has been thoroughly studied. However, robot arms operate in Cartesian space in most cases. Here the dynamics equation in Cartesian space is given as (6). Note that the computation of control laws restricts to joint space in both cases.

$$M_x(q)\ddot{x} + C_x(q, \dot{q})\dot{x} + g_x(q) = J^{\dagger T} \tau + F \quad (6)$$

where

$$\begin{aligned} M_x(q) &= J^{\dagger T}(q) M(q) J^{\dagger}(q) \\ C_x(q, \dot{q}) &= J^{\dagger T}(q) C(q, \dot{q}) J^{\dagger}(q) - J^{\dagger T} M J^{\dagger} \dot{J} J^{\dagger}(q) \\ g_x(q) &= J^{\dagger T}(q) g(q) \end{aligned} \quad (7)$$

J^{\dagger} is pseudoinverse of the Jacobian matrix, which is typically expressed as $J^{\dagger} = J^T(JJ^T)^{-1}$. $M_x(q)$, $C_x(q, \dot{q})$, $g_x(q)$ are the inertia matrix in Cartesian space, Coriolis and Centrifugal forces and gravity expressed in Cartesian space, respectively. A few properties useful for analysis are listed as follows.

Properties

- (i) The inertia matrix $M_x(q) > 0$ or positive definite matrix, provided Jacobian matrix $J(q)$ is nonsingular.

- (ii) The matrix $\dot{M}_x - 2C_x$ is skew-symmetric, provided $\dot{M}_q - 2C(q, \dot{q})$ satisfies the same property.

4.2. Controller Design. Impedance control imposes a desired dynamic behavior to the interaction between robot end-effector and environment, and the desired performance is specified through a generalized dynamic impedance, namely, a complete set of mass-spring-damper equations. Here, the desired dynamic behavior is based on Maxwell model, not typical Voigt ones using by standard impedance control. In other words, dynamic behavior described by (8) is desired in Maxwell model based impedance control.

$$M_d \ddot{x}_e + K_d C_d^{-1} M_d \dot{x}_e + K_d x_e = F + K_d C_d^{-1} \int F dt \quad (8)$$

where M_d is the desired inertia matrix, C_d and K_d are desired damper and spring coefficient matrix, respectively. The last force integral term $K_d C_d^{-1} \int F dt$ should be paid more attention, since it is the main difference between Maxwell model and the traditional Voigt model. Before the impedance controller design, a few prerequisites or assumptions are made here.

Prerequisites

- (i) Jacobian matrix J is nonsingular, which means the prevention of singular is measured and well handled.
- (ii) Feedback information of the external force F . Normally, external forces can be gauged by F/T force sensors or estimated by contact force/torque observers [20].

To achieve the desired response described by (8), a nonlinear feedback control law is derived as the following equation.

$$\begin{aligned} \tau &= M_q J^{\dagger} \left[\ddot{x}_d - M_d^{-1} (K_d C_d^{-1} M_d \dot{x}_e + K_d x_e) \right] + g(q) \\ &+ C(q, \dot{q}) \dot{q} - M_q J^{\dagger} \dot{J} \dot{q} + (M_q J^{\dagger} M_d^{-1} - J^T) F \\ &+ M_q J^{\dagger} M_d^{-1} K_d C_d^{-1} \int F dt \end{aligned} \quad (9)$$

For better understanding, the results above can be divided into several terms, namely, feed-forward term $\tau_{FF} = M_q J^{\dagger} \ddot{x}_d$, nonlinear compensation term $\tau_{NC} = g(q) + C(q, \dot{q}) \dot{q} - M_q J^{\dagger} \dot{J} \dot{q}$, viscoelasticity regulation term $\tau_{VR} = -M_q J^{\dagger} M_d^{-1} (K_d C_d^{-1} M_d \dot{x}_e + K_d x_e)$, inertia shaping term

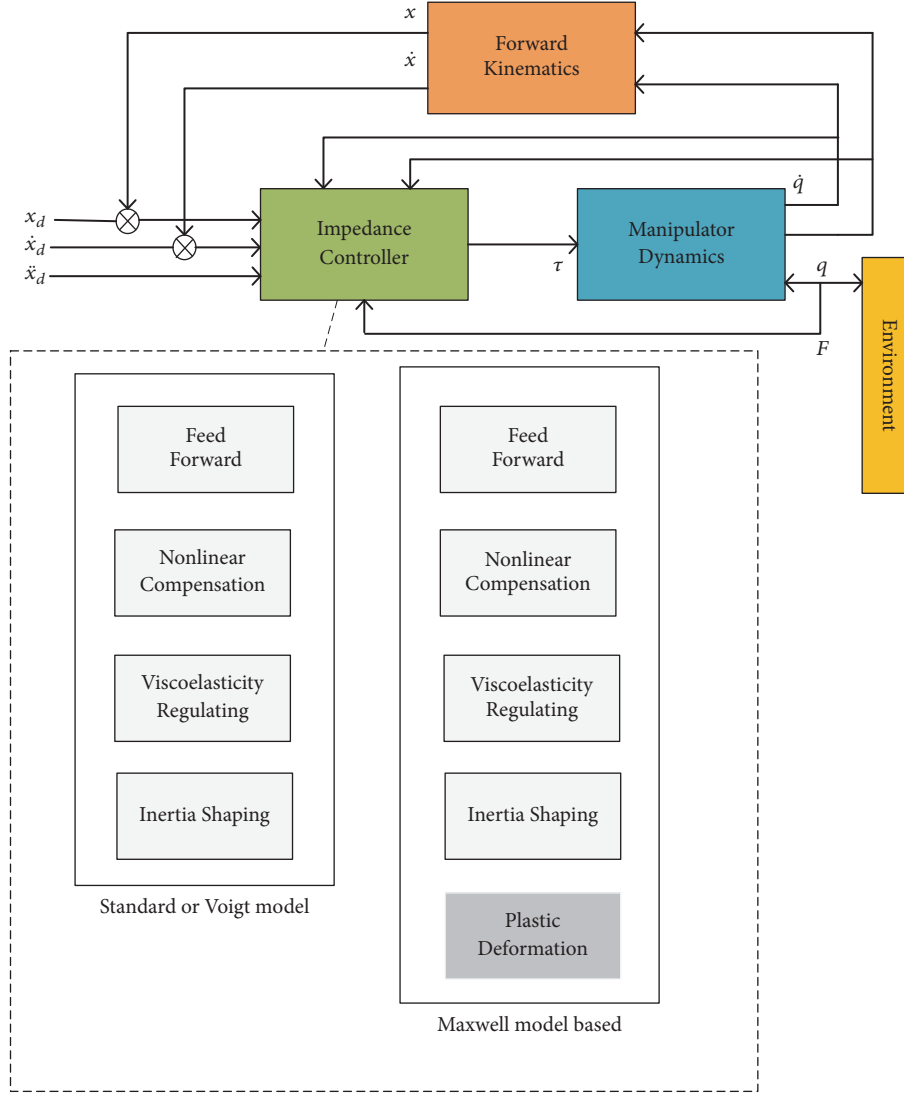


FIGURE 3: Cartesian impedance control architecture of our method and standard impedance control.

$\tau_{IS} = (M_q J^\dagger M_d^{-1} - J^T)F$, and plastic deformation term $\tau_{PD} = M_q J^\dagger M_d^{-1} K_d C_d^{-1} \int F dt$.

The control architecture of both our method and standard impedance control is illustrated in Figure 3. The main differences between our method and the standard impedance control are summarized as follows. On one hand, the external force integral term, which is also called plastic deformation term, $\tau_{PD} = M_q J^\dagger M_d^{-1} K_d C_d^{-1} \int F dt$ is the key part which made our impedance control law different from standard ones. This term is also the cause of plastic deformation of the proposed behavior since this integration does not disappear even after external forces vanish. Moreover, due to the property of integral, accumulations of deviations caused by successive forces exist and are verified by our following experiments. Therefore, it is worth to note that limitations should be added to prevent this integral from becoming saturation or exceed the hard limits of mechanical components in real scenario implementation. On the other hand, derivation of the end-effector goes to zero in standard impedance control

case. In other words, the end-effector returns to its original position after external forces vanish. This elastic behavior can be easily validated theoretically and practically. However, in our case things work in other way. Due to the nonvanish force integral term, the end-effector never goes back to its original position even if friction between structures is not taken into consideration. Besides, this deviation accumulates as external forces continuously exert on the end-effector. That is what plastic elastic deformation means.

Moreover, if gravity is compensated appropriately or in some scenarios such as planar or space robots, the proposed impedance control law can be simplified into the following.

$$\begin{aligned} \tau = & M_q J^\dagger \left[\ddot{x}_d - M_d^{-1} (K_d C_d^{-1} M_d \dot{x}_e + K_d x_e) \right] \\ & + C(q, \dot{q}) \dot{q} - M_q J^\dagger \dot{J} \dot{q} + (M_q J^\dagger M_d^{-1} - J^T) F \\ & + M_q J^\dagger M_d^{-1} K_d C_d^{-1} \int F dt \end{aligned} \quad (10)$$

TABLE 2: Dynamic equations of the 3DOF Planar manipulator.

Variable	Equivalent
$M(1,1)$	$1.04 + 0.08 \cos(q_2 + q_3) + 0.34 \cos(q_2) + 0.05 \cos(q_3)$
$M(1,2)$	$0.43 + 0.04 \cos(q_2 + q_3) + 0.17 \cos(q_2) + 0.05 \cos(q_3)$
$M(1,3)$	$0.17 + 0.04 \cos(q_2 + q_3) + 0.023 \cos(q_3)$
$M(2,2)$	$0.43 + 0.05 \cos(q_3)$
$M(2,3)$	$0.17 + 0.03 \cos(q_3)$
$M(3,3)$	0.17
$F_{friction}$	2.6×10^{-4}

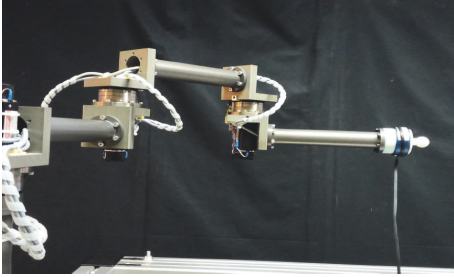


FIGURE 4: Robot manipulator in experiment setting.

In this paper, since a planar robot manipulator is used in our experiment, then Cartesian impedance control law expressed by (10) is our choice.

5. Experiments

The experiment settings in this work are shown in Figure 4. The 3-DOF planar robot manipulator is actuated by three Maxon® motors fixed on the joints with a turn ratio of 1:100. The actuators are installed in parallel along the three axes, such that the redundant robot moves in the horizontal ($X - Y$) plane and gravity in vertical direction (Z) is ignored. Dynamic equations and parameters with International Standard Unit (forces in N , etc.) are listed in Table 2. Remember that Coriolis and Centrifugal terms can be derived via the inertia matrix in the table, and gravity forces are omitted in our planner robot case. The incremental encoders offer the joint position measurement with a resolution of 2000. The sensors and actuators are connected with the computer using a PCI communication card. The Maxon® driver is used to communicate between the executable and the robot. The algorithm proposed is executed in Ubuntu Linux system with RT-Kernel, and the first order Euler solver runs at a sampling rate of 1 kHz. A JR3® 67M series digital output force sensor which can provide up to 6 dimensions of contact force and torque is mounted on the wrist of robot end-effector.

In order to make a comparison between our Maxwell model based method and the standard impedance controller, an experiment of standard Cartesian impedance control is conducted first. The typical elastic deformation is observed and experimental results are given below. After that, experiments of our method have taken place and discussions are

made. The main content of our experiments can be found on the attached video (.mp4).

5.1. Standard Impedance Control in Cartesian Space. The desired impedance are defined as $M_d = \text{diag}[2, 2]Ns^2/m$, $C_d = \text{diag}[30, 30]Ns/m$, and $K_d = \text{diag}[100, 100]N/m$. The time response of external forces exerted on the robot end-effector by human or environment objects is shown in Figure 5(a). And the corresponding deviation of end-effector in Cartesian space is given in Figure 5(b). Since the robot manipulator operates in Cartesian space and it is easier for us to observe its deformation behavior, the joint space displacements are not given here. It turns out that the end-effector returns to its original position even after successive external forces which happen at 17.2s and 21.4s. Besides, there is no accumulated displacement between two external forces. The end-effector goes back directly to Cartesian position $(x_e, y_e) = (-0.07, 0.6)m$ after one external contact force vanishes. This kind of robot behavior is considered as elastic deformation and it is widely used in literatures with respect to impedance control both in joint and Cartesian space.

5.2. Maxwell Model Based Cartesian Impedance Control. Experiments of our method which is Maxwell model based Cartesian impedance control are conducted in several manners. Firstly, experimental results in one external force case with desired impedance parameters $M_d = \text{diag}[2, 2]Ns^2/m$, $C_d = \text{diag}[30, 30]Ns/m$ and $K_d = \text{diag}[100, 100]N/m$ are given in Figure 6. The time response of external force and corresponding Cartesian deviation of end-effector are given in Figures 6(a) and 6(b), respectively. It is shown that the end-effector never returns to its original position $(x_e, y_e) = (-0.07, 0.6)m$ even after the external force vanishes, staying at Cartesian position $(x_e, y_e) = (0.09, 0.58)m$. In other words, the deviations in both x and y directions caused by external contact force exist and remain before next external force comes. This phenomenon is also shown in Figure 6. That is why we call it plastic deformation behavior which is different from elastic deformation shown above.

In Figure 6, it is indicated that larger external forces result in larger deformations in both Cartesian directions. Moreover, Figure 7 shows that the deviation accumulates between two successive external forces. In our view, the internal term of external force $K_d C_d^{-1} \int F dt$ plays a central role in our novel Maxwell model based impedance control method. This force integral term is also the main difference

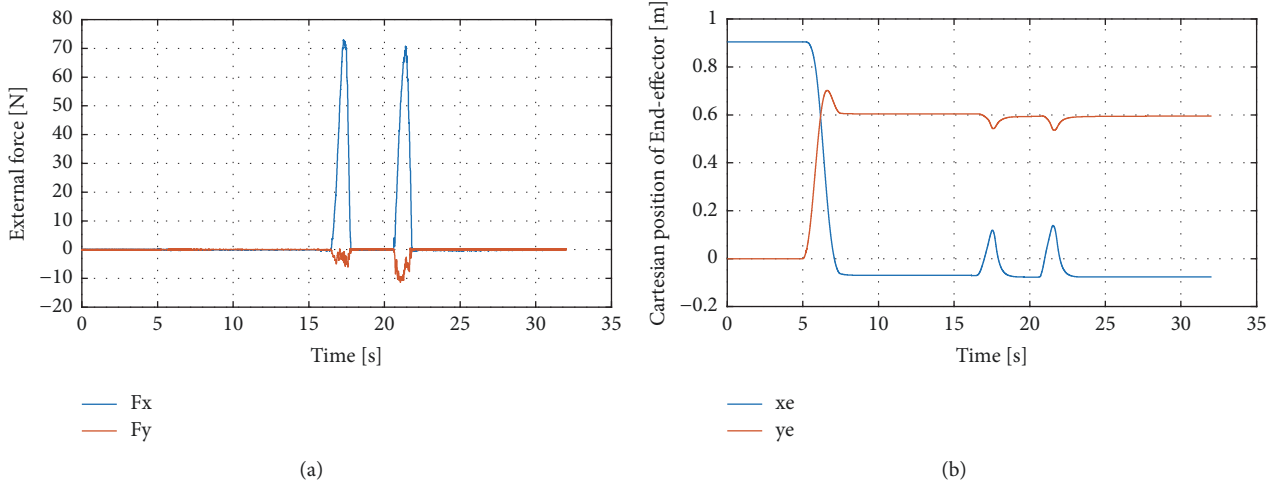


FIGURE 5: Experimental results of standard impedance control. (a) External forces. (b) End-effector position in Cartesian space.

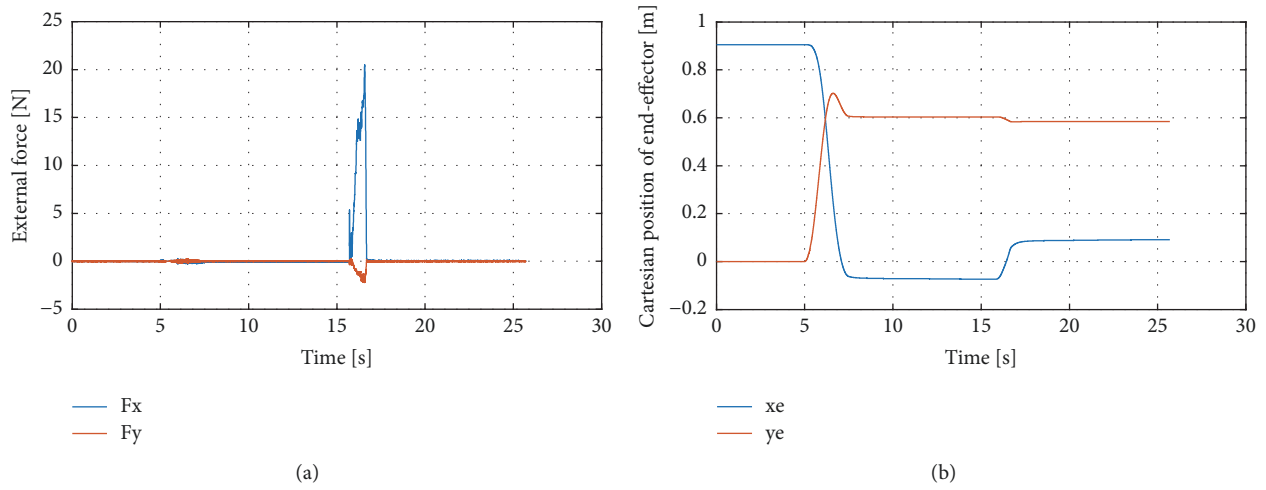


FIGURE 6: Experimental results of Maxwell model based Cartesian impedance control. (a) External force. (b) End-effector position in Cartesian space.

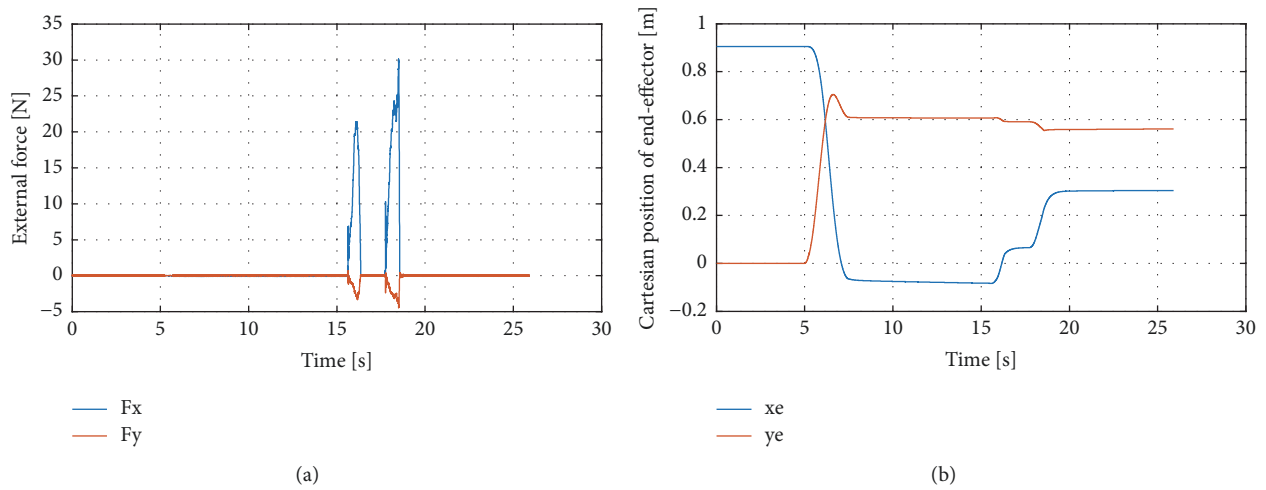


FIGURE 7: Experimental results of Maxwell model based Cartesian impedance control. (a) External forces. (b) End-effector position in Cartesian space.

between our method and the standard or typical impedance control methodology. Because of the inherent property of integration, deviations caused by external forces remain even after the external forces vanish. Besides, these deviations accumulate as the external force goes and may exceed the hardware limits thereby causing damage to robots. Therefore, it is worth to emphasize that saturations of actuators should be taken care of and prevented by taking some measures like setting upper limits in real robot implementations.

6. Conclusions

A novel Cartesian impedance controller based on Maxwell model is designed and implemented practically in a robot manipulator platform. Both viscosity models are analyzed and the equivalent transformation between them is given. By contrast, this novel kind of impedance control makes the robot endure a plastic deformation behavior which is highly different from standard elastic deformation. Certain extent compliance is achieved under unpredictable contact forces. Our work shows a promising usage in some tasks such as robot catching flying ball without repelling. Moreover, this kind of compliance may open a gate in human robot collaboration tasks to ensure a more soft and passive physical interaction between robot and human.

Data Availability

The data used to support the findings of this study are available from the corresponding author upon request.

Conflicts of Interest

The authors declare that they have no conflicts of interest.

Acknowledgments

The project is supported by the Major Research Plan (Grant No. 91648201) and the Foundation for Innovative Research Groups (Grant No. 51521003) of the National Natural Science Foundation of China.

Supplementary Materials

The video attachment is a supplementary material of this research article. This video file also serves as a verification and demonstration of our work. This video (.mp4) is in the well-known MPEG-4 format. No special requirements for video player. Generally, there are three parts in this video. At the beginning, standard Cartesian impedance control is implemented as a comparison work. A typical elastic deformation behavior is observed when external forces applied. After that, the experiment using our method which is called Maxwell model based Cartesian impedance control is demonstrated. A plastic deformation behavior is clearly observed when the robot physically interacts with human. The last part is called "Fried Potato Chip Test" in which a human applies contact forces via fragile potato chips. Small forces cause accumulated deviations of the end-effector. In short, a plastic deformation

behavior is practically implemented in a robot manipulator platform by using our novel Maxwell model based Cartesian impedance control. (*Supplementary Materials*)

References

- [1] J. D. Lane, "Evaluation of a remote center compliance device," *Assembly Automation*, vol. 1, no. 1, pp. 36–46, 1980.
- [2] S. Wolf and G. Hirzinger, "A new variable stiffness design: Matching requirements of the next robot generation," in *Proceedings of the 2008 IEEE International Conference on Robotics and Automation, ICRA 2008*, pp. 1741–1746, USA, May 2008.
- [3] K. Koganezawa, "Mechanical stiffness control for antagonistically driven joints," in *Proceedings of the IEEE IRS/RSJ International Conference on Intelligent Robots and Systems, IROS 2005*, pp. 1544–1551, IEEE, Canada, August 2005.
- [4] C.-P. Chou and B. Hannaford, "Measurement and modeling of McKibben pneumatic artificial muscles," *IEEE Transactions on Robotics and Automation*, vol. 12, no. 1, pp. 90–102, 1996.
- [5] A. Bicchi, S. L. Rizzini, and G. Tonietti, "Compliant design for intrinsic safety: General issues and preliminary design," in *Proceedings of the 2001 IEEE/RSJ International Conference on Intelligent Robots and Systems*, pp. 1864–1869, USA, November 2001.
- [6] N. Hogan, "Impedance control: an approach to manipulation," in *Proceedings of the American Control Conference*, pp. 304–313, IEEE, 1984.
- [7] N. Hogan, "Impedance control: an approach to manipulation: part II—implementation," *Journal of Dynamic Systems, Measurement, and Control*, vol. 107, no. 1, pp. 8–16, 1985.
- [8] J. Salisbury, "Active stiffness control of a manipulator in cartesian coordinates," in *Proceedings of the 1980 19th IEEE Conference on Decision and Control including the Symposium on Adaptive Processes*, pp. 95–100, Albuquerque, NM, USA, December 1980.
- [9] M. Kaneko, K. Yokoi, and K. Tanie, "Direct Compliance Control for Serial Link Arm: (1st Report, Basic Concept and Decoupling Condition)," *Transactions of The Japan Society of Mechanical Engineers Series C*, vol. 54, no. 503, pp. 1510–1514, 1988.
- [10] B. Siciliano, "Kinematic control of redundant robot manipulators: A tutorial," *Journal of Intelligent & Robotic Systems*, vol. 3, no. 3, pp. 201–212, 1990.
- [11] A. Albu-Schäffer, C. Ott, U. Frese, and G. Hirzinger, "Cartesian impedance control of redundant robots: Recent results with the DLR-Light-Weight-Arms," in *Proceedings of the 2003 IEEE International Conference on Robotics and Automation*, pp. 3704–3709, Taiwan, September 2003.
- [12] A. Albu-Schäffer, C. Ott, and G. Hirzinger, "A unified passivity-based control framework for position, torque and impedance control of flexible joint robots," *International Journal of Robotics Research*, vol. 26, no. 1, pp. 23–39, 2007.
- [13] C. Ott, A. Albu-Schäffer, A. Kugi, and G. Hirzinger, "On the passivity-based impedance control of flexible joint robots," *IEEE Transactions on Robotics*, vol. 24, no. 2, pp. 416–429, 2008.
- [14] Y. Li, S. S. Ge, and C. Yang, "Learning impedance control for physical robot-environment interaction," *International Journal of Control*, vol. 85, no. 2, pp. 182–193, 2012.
- [15] C. Yang, C. Zeng, P. Liang, Z. Li, R. Li, and C.-Y. Su, "Interface Design of a Physical Human-Robot Interaction System for Human Impedance Adaptive Skill Transfer," *IEEE Transactions*

- on Automation Science and Engineering*, vol. 15, no. 1, pp. 329–340, 2018.
- [16] C. Yang, C. Zeng, C. Fang, W. He, and Z. Li, “A DMPs-based Framework for Robot Learning and Generalization of Human-like Variable Impedance Skills,” *IEEE/ASME Transactions on Mechatronics*, vol. 23, no. 3, pp. 1193–1203, 2018.
- [17] T. W. Spriggs, J. D. Huppler, and B. R. Bird, “An experimental appraisal of viscoelastic models,” *Transactions of the Society of Rheology*, vol. 10, no. 1, pp. 191–213, 1966.
- [18] T. Senoo, M. Koike, K. Murakami, and M. Ishikawa, “Visual shock absorber based on maxwell model for anti-rebound control,” in *Proceedings of the IEEE/RSJ International Conference on Intelligent Robots and Systems, IROS 2015*, pp. 1640–1645, Germany, October 2015.
- [19] T. Senoo, M. Koike, K. Murakami, and M. Ishikawa, “Impedance Control Design Based on Plastic Deformation for a Robotic Arm,” *IEEE Robotics and Automation Letters*, vol. 2, no. 1, pp. 209–216, 2017.
- [20] G. Bätz, B. Weber, M. Scheint, D. Wollherr, and M. Buss, “Dynamic contact force/torque observer: Sensor fusion for improved interaction control,” *International Journal of Robotics Research*, vol. 32, no. 4, pp. 446–457, 2013.




Hindawi

Submit your manuscripts at
www.hindawi.com

